

**Roles of a short connecting disulfide bond in the stability and function of psychrophilic**

*Shewanella violacea* cytochrome  $c_5$ \*<sup>\*</sup>

**Keiko Ogawa<sup>1</sup> · Takafumi Sonoyama<sup>1</sup> · Taku Takeda<sup>1</sup> · Shin-ichi Ichiki<sup>1</sup> · Shota**

**Nakamura<sup>2</sup> · Yuji Kobayashi<sup>2</sup> · Susumu Uchiyama<sup>3</sup> · Kaoru Nakasone<sup>4</sup> · Shin-ichi J.**

**Takayama<sup>5</sup> · Hajime Mita<sup>5</sup> · Yasuhiko Yamamoto<sup>5</sup> · Yoshihiro Sambongi<sup>1,\*</sup>**

<sup>1</sup>Graduate School of Biosphere Science, Hiroshima University, CREST of Japan Science and Technology Corporation, 1-4-4 Kagamiyama, Higashi-Hiroshima, Hiroshima 739-8528, Japan.

<sup>2</sup>Graduate School of Pharmaceutical Sciences, Osaka University, Suita 565-0871, Japan.

<sup>3</sup>Graduate School of Engineering, Osaka University, Suita 565-0871, Japan.

<sup>4</sup>Department of Chemistry and Environmental Technology, School of Engineering, Kinki University, Umenobe Takaya 1, Higashi-Hiroshima, Hiroshima 739-2116, Japan.

<sup>5</sup>Department of Chemistry, University of Tsukuba, Tsukuba 305-8571, Japan.

\*Corresponding author. Fax: +81-82-424-7924, E-mail: sambongi@hiroshima-u.ac.jp

**Abbreviations** SV cytc<sub>5</sub>, *Shewanella violacea* mono-heme cytochrome  $c_5$  · CD, circular dichroism · CV, cyclic voltammetry · DSC, differential scanning calorimetry · PCR, polymerase chain reaction · SDS, sodium dodecyl sulfate

**Abstract** Cys-59 and Cys-62, forming a disulfide bond in the four-residue loop of *Shewanella violacea* cytochrome  $c_5$  (SV  $cyt_{c_5}$ ), contribute to protein stability but not to redox function.

These Cys residues were substituted with Ala in SV  $cyt_{c_5}$ , and the structural and functional properties of the resulting C59A/C62A variant were determined and compared with those of the wild-type. The variant had similar features to those of the wild-type in absorption, circular dichroic, and paramagnetic  $^1\text{H}$  NMR spectra. In addition, the redox potentials of the wild-type and variant were essentially the same, indicating that removal of the disulfide bond from SV  $cyt_{c_5}$  does not affect the redox function generated in the vicinity of heme. However, calorimetric analysis of the wild-type and variant showed that the mutations caused a drastic decrease in the protein stability through enthalpy, but not entropy. Four residues are encompassed by the SV  $cyt_{c_5}$  disulfide bond, which is the shortest one that has been proved to affect protein stability. The protein stability of SV  $cyt_{c_5}$  can be controlled without changing the redox function, providing a new strategy for regulating the stability and function of cytochrome  $c$ .

**Keywords** cytochrome  $c$  · *Shewanella violacea* · disulfide bond · protein stability · redox potential · psychrophiles

## Introduction

The disulfide bond is one of the crucial elements determining protein structure (Betz 1993). In various proteins such as azurin (Guzzi et al. 1999; Bonander et al. 2000) and lysozyme (Kuroki et al. 1992; Kidera et al. 1994), the integrity of the three-dimensional structure is due to the presence of disulfide bonds, because the removal of naturally occurring bonds results in a reduction of the protein stability. Disulfide bonds also affect the protein folding pathway and kinetics, for example, as observed in the constant domain of the antibody light chain (Goto and Hamaguchi 1982; Feige et al. 2007). In addition to these effects on protein stability and folding, the formation of disulfide bonds correlates with the redox function of the membrane-bound cytochromes (cyts)  $c_1$  from some photosynthetic bacteria (Osyczka et al. 2001; Elberry et al. 2006).

Mono-heme soluble class I cyts  $c$  have been used as model proteins in various areas of protein science (Sambongi et al. 2002). Nonetheless, using class I cyts  $c$ , structural and functional aspects involving the disulfide bond have not been examined in detail, partly because the presence of disulfide bonds is uncommon in this protein family. A class I cyt  $c$  with a single disulfide bond formed from two considerably separated Cys residues in the primary sequence is seldom found in living systems, those of bullfrog (Brems et al. 1982) and *Methylobacterium extorquens* (Williams et al. 2006) being rare examples. Other examples of

class I cyts *c* with disulfide bonds are *Arabidopsis thaliana* cyt *c*<sub>6A</sub> (Chida et al. 2006; Marcaida et al. 2006), *Azotobacter vinelandii* cyt *c*<sub>5</sub> (AV cyt<sub>c5</sub>, Carter et al. 1985), and *Shewanella oneidensis* cyt *c*<sub>5</sub> (original bacterial name, *Shewanella putrefaciens*; and protein name, ScyA, Bartalesi et al. 2002). Three-dimensional structure analysis showed that these three proteins each have a short connecting disulfide bond in a loop region of the polypeptide chain on the C-terminal side of the Met residue coordinating with the heme iron as the sixth axial ligand.

Genome analysis showed that the sequences of the cyts *c* from some *Shewanella* species are more than 70 % identical to the ScyA sequence and seem to have a disulfide bond because they contain two conserved Cys residues corresponding to those forming the bond in ScyA. A recent detailed bioinformatics study (Bertini et al. 2006) indicated that the *Shewanella* cyts *c* belong to Ambler's class IE (Ambler 1991), which also includes AV cyt<sub>c5</sub>. The disulfide bond found in class IE cyts *c* always connects the shortest length of polypeptide chain: only two amino acid residues intervene in the bond in the four-residue short loop. The thermodynamic and functional effects of such a short connecting disulfide bond have not been elucidated so far.

Mono-heme cyt *c*<sub>5</sub> (SV cyt<sub>c5</sub>) from a psychrophilic and piezophilic Gram-negative bacterium, *Shewanella violacea* (Nogi et al. 1998), is a class IE cyt *c*. SV cyt<sub>c5</sub> was designated as a cyt *c*<sub>A</sub> containing one heme per polypeptide in the previous report (Yamada et al. 2000). In this study, the structural, thermodynamic, and functional consequences of removal of the

short connecting disulfide bond from SV *cytc*<sub>5</sub> were investigated. For this purpose, we cloned the gene encoding SV *cytc*<sub>5</sub> and established an expression system for it using *E. coli* as a host. The two Cys residues forming the disulfide bond in SV *cytc*<sub>5</sub> were substituted with Ala, and the resulting variant and the wild-type were analyzed.

## **Materials and methods**

### Growth of *S. violacea*, and preparation of DNA and periplasmic extracts

*S. violacea* DSS12 (JCM10179), isolated from deep-sea sediment obtained from the Ryukyu Trench at a depth of 5,110 m, was used in this study. The *S. violacea* cells were grown in the liquid medium marine broth 2216 (Difco) at 8 °C as described previously (Nogi et al. 1998).

Chromosomal DNA was extracted from the *S. violacea* cells by the standard method, and used as a template for the PCR (polymerase chain reaction) experiment. Periplasmic extracts were obtained from the *S. violacea* cells by the cold osmotic shock method (Sambongi et al. 1996), and authentic SV *cytc*<sub>5</sub> was purified from them.

### Isolation of the SV *cytc*<sub>5</sub> gene and its expression

After publication of the DNA sequence of *S. violacea* cyt  $c_A$  (Yamada et al. 2000), which is here renamed SV  $cytc_5$ , we realized that the published sequence contains an error. Therefore, we again screened a *S. violacea* DSS12  $\lambda$  phage library (Yamada et al. 2000) using the original clone of the cyt  $c_A$  gene as a hybridization probe, and the resulting positive clone was sequenced. We have deposited the revised sequence of the SV  $cytc_5$  gene under DDBJ accession number AB032404.

Based on the revised sequence, we designed PCR primers to amplify the gene encoding the mature SV  $cytc_5$ . The amplified gene was fused with the gene for the signal sequence of *Pseudomonas aeruginosa* cyt  $c_{551}$  (PA  $c_{551}$ ) in the 5' region (Zhang et al. 1998), and then the fusion gene was inserted into the pKK223-3 vector (ampicillin resistance) under the control of the *tac* promoter. The resulting plasmid was designated as pOK3. Into the fusion gene, mutations of Cys-59 to Ala and Cys-62 to Ala (C59A/C62A) were introduced by a PCR-based method as described previously (Hasegawa et al. 1999). The resulting mutated SV  $cytc_5$  gene with the PA  $c_{551}$  signal sequence was inserted into the pKK223-3 vector. Plasmid pEC86 (chloramphenicol resistance), carrying the *ccmABCDEFGH* genes for cyt  $c$  maturation proteins (Arslan et al. 1998), was co-transformed into *E. coli* JCB387 together with pOK3 or its derivative carrying the mutated SV  $cytc_5$  gene.

## Preparation of SV *cyt<sub>c5</sub>* protein

*E. coli* JCB387 cells carrying both pEC86 and pOK3, or pOK3 derivative were initially grown in the liquid Luria-Bertani medium containing 100  $\mu\text{g mL}^{-1}$  ampicillin and 34  $\mu\text{g mL}^{-1}$  chloramphenicol. The resulting cultures (20 mL) were inoculated into 2 L of minimal medium containing 0.4 % glycerol, as a carbon source, and the two antibiotics in 5 L flasks, which were then shaken aerobically at 37 °C for an appropriate period before harvesting as described previously (Oikawa et al. 2005).

Periplasmic extracts of the resulting *E. coli* cells carrying the SV *cyt<sub>c5</sub>* gene were obtained by the cold osmotic shock method (Sambongi et al. 1996). The recombinant SV *cyt<sub>c5</sub>* protein in the periplasmic extract was purified by Hi Trap Q column chromatography (Amersham Pharmacia Biotech), with elution with 10 mM Tris-HCl buffer (pH 8.0) containing an NaCl concentration gradient (0 – 500 mM), followed by chromatography on a Superdex 75 column equilibrated and eluted with 25 mM sodium acetate buffer (pH 5.0). The authentic SV *cyt<sub>c5</sub>* protein was also purified by the same method from a *S. violacea* periplasmic extract. The protein's purity was confirmed by sodium dodecyl sulfate (SDS) polyacrylamide gel electrophoresis followed by staining with Coomassie Brilliant Blue.

Absorption, circular dichroic, and paramagnetic  $^1\text{H}$  NMR spectroscopy

Absorption and circular dichroic (CD) spectra of the SV cyt<sub>c5</sub> wild-type and C59A/C62A variant (20 or 100 μM) in 20 mM sodium acetate buffer (pH 5.0) were measured with a JASCO V-530 spectrophotometer and a JASCO J-820 spectrometer, respectively. Paramagnetic <sup>1</sup>H NMR spectra of oxidized SV cyt<sub>c5</sub> were recorded at pH 7.2 on a Bruker AVANCE-600 spectrometer (the Chemical Analysis Center, University of Tsukuba) operating at the <sup>1</sup>H frequency of 600 MHz (Terui et al. 2003). The protein concentration for the <sup>1</sup>H NMR measurements was approximately 1 mM in 90 % H<sub>2</sub>O/ 10 % <sup>2</sup>H<sub>2</sub>O. Chemical shifts are given in ppm downfield from sodium 2,2-dimethyl-2-silapentane-5-sulfonate with the residual H<sup>2</sup>O as an internal reference. All of these spectral analyses were carried out at 25 °C.

#### Protein denaturation

Thermal denaturation experiments were carried out by monitoring CD in a pressure-proof cell compartment (JASCO), which was attached to a JASCO J-820 CD spectrometer (Uchiyama et al. 2004). This apparatus facilitated thermal denaturation measurement up to 180 °C under the pressure of 10 atm. Protein solutions of the air-oxidized SV cyt<sub>c5</sub> wild-type and C59A/C62A variant (20 μM) in 20 mM sodium acetate buffer (pH 5.0) were subjected to the following analysis. The temperature-dependent CD ellipticity change at 222 nm was followed in cuvettes of 1 mm path-length. The CD values were recorded from 25 to 120 °C with a heating



rate of  $1\text{ }^{\circ}\text{C min}^{-1}$ . The raw data were subjected to nonlinear least-squares fitting with MATHEMATICA 3.0 as described previously (Uchiyama et al. 2004), and the resulting thermal denaturation curves were used to determine the temperature at the midpoint of the transition ( $T_{m,CD}$ ). The enthalpy change during thermal denaturation ( $\Delta H_{vH}$ ) was calculated on the basis of van't Hoff analysis.

Thermal denaturation experiments involving differential scanning calorimetry (DSC) were also carried out. The solutions of air-oxidized SV cytc<sub>5</sub> wild-type and C59A/C62A variant were dialyzed extensively against 20 mM sodium acetate buffer (pH 5.0) before the measurements. The degassed protein solutions ( $\sim 100\text{ }\mu\text{M}$ ) were then loaded into a calorimeter cell and heated from 10 to 120  $^{\circ}\text{C}$  at  $\sim 28\text{ psi}$ , at the heating rate of  $1\text{ }^{\circ}\text{C min}^{-1}$ , with a calorimeter VP-DSC (Microcal Inc., MA, USA). Buffer-buffer base lines were recorded at the same heating rate and then subtracted from the sample curves to obtain the heat capacity ( $C_p$ ) curves. After fitting the data with MATHEMATICA 3.0, the transition temperature during thermal denaturation ( $T_m$ ) and the calorimetric enthalpy change ( $\Delta H_{cal}$ ) at  $T_m$  were obtained. The heat capacity change accompanied by the thermal denaturation,  $\Delta C_p$ , was estimated as a function of temperature as described previously (Uchiyama et al. 2002). From these values, thermodynamic parameters [free energy change ( $\Delta G$ ), enthalpy change ( $\Delta H$ ), and entropy change ( $\Delta S$ )] at a given temperature were calculated using the following equations:

$$\Delta H(T) = \Delta H_{\text{cal}} - \Delta C_p(T)(T_m - T)$$

$$\Delta S(T) = \Delta H_{\text{cal}}/T_m - \Delta C_p(T) \ln(T_m/T)$$

$$\Delta G(T) = \Delta H(T) - T\Delta S(T)$$

These calculations facilitated comparison of the thermodynamic protein stability as described previously (Uchiyama et al. 2002).

Guanidine hydrochloride (GdnHCl) denaturation measurement by means of CD was carried out according to the previously described method (Hasegawa et al. 1999). The air-oxidized SV cyt<sub>c</sub>5 wild-type and C59A/C62A variant (20 μM) were incubated in 20 mM sodium acetate buffer (pH 5.0) with varying concentrations of GdnHCl at 25 °C for 2 h before the measurements in order to equilibrate the proteins with the denaturant. The CD ellipticity at 222 nm of the protein solution was measured using a 1 mm path-length cuvette at 25 °C. The free energy change in H<sub>2</sub>O ( $\Delta G_{\text{H}_2\text{O}}$ ) and the dependence of  $\Delta G$  on the GdnHCl concentration ( $m$ ) were determined by nonlinear least-squares fitting of the data from the transition region using the equation  $\Delta G = \Delta G_{\text{H}_2\text{O}} - m[\text{GdnHCl}]$  (Pace 1990). The midpoint concentration of denaturation ( $C_m$ ) was the GdnHCl concentration at which the  $\Delta G$  value became zero.

### Cyclic voltammetry

The procedures used for obtaining cyclic voltammograms (CV) of the SV cyt<sub>c</sub>5 wild-type and

variant were essentially the same as those described previously (Terui et al. 2003). CV experiments were performed with a Potentiostat-Galvanostat PGSTAT12 (Autolab, Netherlands). A glassy carbon electrode (GCE) was polished with 0.05  $\mu\text{m}$  alumina slurry and then sonicated in a deionized water bath for 1 min. The protein solutions of SV *cytc*<sub>5</sub> wild-type and C59A/C62A variant (2  $\mu\text{l}$ , 1 mM) in 20 mM phosphate buffer, pH 6.0, were spread evenly with a microsyringe over the surface of the GCE. Then the GCE surface was covered with a semipermeable membrane. An Ag | AgCl electrode in a saturated NaCl solution and a Pt wire were employed as the reference and counter electrodes, respectively. The potential sweep range was +350 to -150 mV vs. the Ag | AgCl electrode in a saturated NaCl solution with a scan rate of 20 mV s<sup>-1</sup>. Potentials were referenced to the standard hydrogen electrode. All experiments were performed at 25 °C under a N<sub>2</sub> atmosphere.

#### Other procedures

The SV *cytc*<sub>5</sub> contents of the *E. coli* and *S. violacea* periplasmic extracts were determined by measuring absorption spectra of solutions to which a few grains of solid sodium dithionite had been added. The extinction coefficient for reduced SV *cytc*<sub>5</sub> at 553 nm, 19,300 M<sup>-1</sup> cm<sup>-1</sup>, was used to calculate the concentrations of both the wild-type and variant. The N-terminal sequence of the recombinant SV *cytc*<sub>5</sub> expressed in the *E. coli* periplasm was determined by

automated Edman sequencing using a peptide sequencer (Hewlett Packard). Activity staining after SDS polyacrylamide gel electrophoresis for heme covalently attached to the polypeptide was also performed (Goodhew et al. 1986). The protein concentrations were estimated by the Bradford method (Bradford 1976) using bovine serum albumin as a standard.

## Materials

The reagents for DNA handling were purchased from Takara Shuzou or Toyobo. GdnHCl (Ultra Pure) was purchased from Nacalai Tesque. All other chemicals used were of the highest grade commercially available.

## Results and discussion

### Sequence analysis of SV *cyt<sub>c5</sub>*

A protein-protein BLAST (Basic Local Alignment Search Tool) search showed that the revised SV *cyt<sub>c5</sub>* sequence exhibited more than 70 % identity with those of the *cyts c* from *Shewanella frigidimarina* NCIMB 400, *Shewanella oneidensis* MR-1, *Shewanella amazonensis* SB2B, *Shewanella putrefaciens* CN-32, *Shewanella baltica* OS155, and *Shewanella denitrificans*

OS217 (Fig. 1). All of these *Shewanella* cyts *c* in the genome sequence database have two conserved Cys residues near the C-terminus besides those in the heme binding motif, Cys-X-X-Cys-His, near the N-terminus (Fig. 1). Among these *Shewanella* cyts *c*, the solution structure of cyt *c* (ScyA) of *S. oneidensis* MR-1 (named *S. putrefaciens* in the original paper) has been determined by NMR (Bartalesi et al. 2002), which showed that the two conserved Cys residues near the C-terminus form a disulfide bond even in the presence of a heme iron reductant, sodium dithionite (Fig. 2A).

#### Expression of SV cytc<sub>5</sub> in the *E. coli* periplasm

The recombinant SV cytc<sub>5</sub> wild-type expressed in *E. coli* JCB387 cells was fully recovered in the periplasmic extract after cold osmotic shock, but not in the membrane and cytoplasmic fractions. The expressed protein had covalently attached heme, as judged on heme activity staining following separation by SDS polyacrylamide gel electrophoresis (data not shown).

The C59A/C62A variant was similarly expressed.

The N-terminal amino acid sequence of the recombinant SV cytc<sub>5</sub> expressed in the *E. coli* periplasm was determined to be Gln-Glu-Gly-Lys-Ala, which is identical to that of the authentic protein purified from the native organism, *S. violacea* (Yamada et al. 2000). This indicates that the PA<sub>c551</sub> signal peptide in the present fusion protein was correctly processed in the *E. coli*

cells. A similar attempt has been already made, the recombinant ScyA being expressed in the *E. coli* periplasm, in which the signal peptide of *E. coli* *cyt b*<sub>562</sub> was used to target the protein to the periplasm (Bartalesi et al. 2002). In that case, three amino acid residues of the signal peptide were left at the N-terminus of the processed ScyA protein, a non-natural *cyt c* being yielded. It is possible that these extra residues affect the thermodynamic properties of ScyA, as exemplified by a recombinant *cyt c* with an N-terminal extra Met residue exhibiting reduced protein stability compared with the authentic protein (Zhang et al. 1998). Since the present recombinant SV *cyt*<sub>5</sub> expressed in the *E. coli* periplasm has an N-terminal sequence identical to the authentic one, the protein stability assay with the recombinant should adequately reflect the properties of the natural protein.

From aerobically growing *E. coli* cells in the stationary phase, 4,000 µg of recombinant SV *cyt*<sub>5</sub> was purified from one liter of culture, which was much more than the only 6 µg of the authentic SV *cyt*<sub>5</sub> from the *S. violacea* cells. The high production of the recombinant SV *cyt*<sub>5</sub> may be due to (i) that the PA *c*<sub>551</sub> signal peptide can target the apo-precursor protein efficiently to the *E. coli* periplasm, and (ii) that the *ccm* genes on the plasmid can be constitutively expressed under aerobic conditions where the *E. coli* growth yield is higher than that under anaerobic ones. The efficient production and easy purification from the *E. coli* periplasm enabled us to obtain a large amount of correctly processed SV *cyt*<sub>5</sub>, which will

facilitate further structural and mutagenesis studies, as described below.

#### Presence of a disulfide bond in the SV *cyt<sub>c</sub>5* wild-type

From the bioinformatics point of view (Bertini et al. 2006), SV *cyt<sub>c</sub>5* can be characterized by the presence of a disulfide bond. Since the SV *cyt<sub>c</sub>5* sequence shows 72 % overall identity with that of structurally characterized ScyA (Bartalesi et al. 2002), it is likely that these two proteins have almost identical main chain conformations. In addition, these two proteins show higher sequence identity around Cys-59 and Cys-62 (Fig. 1). Therefore, as indicated by the bioinformatics study, the SV *cyt<sub>c</sub>5* wild-type has a similar disulfide bond to ScyA.

The presence of a disulfide bond in the SV *cyt<sub>c</sub>5* wild-type can be experimentally inferred from the results of SDS polyacrylamide gel electrophoresis. After boiling the samples for 5 min with 100 mM dithiothreitol (DTT) and 1 % SDS, the mobility of the purified wild-type and C59A/C62A variant in the SDS gel was the same (Fig. 3), indicating that the two proteins are highly alike in the same unfolded state. In contrast, without the boiling and DTT treatment, the wild-type migrated faster than the variant in the SDS gel (Fig. 3). Although the protein amounts applied to the SDS gel were the same, the DTT-**untreated** wild-type band was less efficiently stained compared with the others. These results are due to the presence of the Cys-59–Cys-62 disulfide bond in the SV *cyt<sub>c</sub>5* wild-type, which partially retains its

conformation even in the SDS gel. The mobility on SDS gels, as presented here, is often examined to see whether a protein contains a disulfide bond or not even if the bond connects a short length of amino acid chain (Akiyama et al. 1992).

### Spectroscopic features

The absorption spectra (400 – 600 nm) of the recombinant SV *cyt<sub>c5</sub>* wild-type showed maxima at 410 nm in the air-oxidized form (Fig. 4A), and at 419, 525, and 553 nm in the dithionite-reduced form (Fig. 4B). These spectral features are completely identical with those of the authentic SV *cyt<sub>c5</sub>* protein purified from *S. violacea* cells (Yamada et al. 2000). This result suggests that the recombinant SV *cyt<sub>c5</sub>* is correctly formed in the *E. coli* periplasm and becomes indistinguishable from the authentic protein.

To see the effect of the C59A/C62A mutations on the SV *cyt<sub>c5</sub>* structure, we performed several spectroscopic measurements for the recombinant SV *cyt<sub>c5</sub>* wild-type and variant. The recombinant C59A/C62A variant exhibited the same absorption as that of the wild-type in both the oxidized and dithionite-reduced forms (Fig. 4, A and B). **The both reduced SV *cyt<sub>c5</sub>* wild-type and variant were not autooxidized under the present conditions.** Furthermore, the wild-type and variant each gave an Fe(III)-S(Met) charge transfer band at 620 nm in their oxidized forms (Fig. 4A, inset). This 620 nm-absorption has been similarly observed for ScyA



(Bartalesi et al. 2002), but not for other cyts *c* such as PA *c*<sub>551</sub>, for which 695 nm-absorption was observed as a charge transfer band.

Far-UV (190 – 250 nm) and near-UV (250 – 400 nm) CD spectra were measured to analyze the secondary and tertiary structures of the SV cyt<sub>c</sub><sub>5</sub> wild-type and C59A/C62A variant, respectively. The spectra (Fig. 4, C and D) revealed that the wild-type and variant had the same minima and maxima, indicating that they had similar secondary and tertiary structures.

Oxidized cyts *c* generally exhibit paramagnetically shifted <sup>1</sup>H NMR signals, providing with information on the heme electronic structure, and the coordination bonds between the heme iron and axial ligands from His and Met residues. The paramagnetic <sup>1</sup>H NMR spectra of the oxidized forms of the SV cyt<sub>c</sub><sub>5</sub> wild-type and C59A/C62A variant showed almost identical shift patterns with signals a – d (as indicated in Fig. 5), which seemed to be derived from heme peripheral methyl protons, and signal e, derived from iron-coordinated Met side chain methyl protons (Fig. 5). This assignment is based on the results of analysis of their line widths in terms of the distances between the heme iron and the protons of interest (Swift 1973): the value of ~6.8 for the ratio of the line widths of signals a – d (~250 Hz) and e (1700 Hz) is consistent with the value of ~6.9 estimated considering the paramagnetic relaxation for the heme methyl and iron-coordinated Met side chain methyl protons located at ~5.1 and ~3.7 Å from the heme iron, respectively.

Although the patterns of paramagnetically shifted  $^1\text{H}$  NMR signals were the same for the SV *cyt<sub>c</sub>5* wild-type and variant, we found some differences in the line shapes of the resolved signals in the downfield regions. Signals c, d, f and g each split into two with an intensity ratio of ~2:1 in the spectrum of the SV *cyt<sub>c</sub>5* wild-type (Fig. 5). In contrast, such splitting was not observed for the corresponding signals of the C59A/C62A variant. These results suggest that conformational heterogeneity occurs around the heme peripheral methyl groups of the SV *cyt<sub>c</sub>5* wild-type, but not in the variant. However, signal e derived from the iron-coordinated Met side chain methyl proton was the same for the wild-type and variant. Therefore, the structure of the heme active site in SV *cyt<sub>c</sub>5* may be independent of the removal of the disulfide bond, His and Met side chains being similarly coordinated to the heme iron as axial ligands in the wild-type and variant.

Taken together, the above absorption, CD, and  $^1\text{H}$  NMR spectral analyses suggest that the removal of the disulfide bond from SV *cyt<sub>c</sub>5* does not significantly affect the protein structure or heme environment at 25 °C, at which the spectral measurements were carried out.

#### Unusual hyperfine shifts

For most oxidized mono-heme cyts *c*, paramagnetically shifted  $^1\text{H}$  NMR signals are observed in the chemical shift range of ~-40 – ~40 ppm. However, in the downfield shifted regions of the

spectra of the SV *cyt<sub>c5</sub>* wild-type and C59A/C62A variant, signals a – e in Fig. 5 were resolved at > 40 ppm. Signals exhibiting shifts as large as 40 ppm were also observed in the spectrum of oxidized ScyA, which have been attributed to the admixture of low and high spin states (Bartalesi et al. 2002). These unusual spectral properties of SV *cyt<sub>c5</sub>* and ScyA will provide a chance to investigate the diversity of the heme environment among cyts *c*. Our present mutation study at least demonstrated that removal of the disulfide bond from SV *cyt<sub>c5</sub>* did not affect the heme environment revealed by these unusual paramagnetic <sup>1</sup>H NMR signals.

Thermal denaturation of oxidized forms measured by CD

Throughout this study, protein stability measurements were carried out with air-oxidized states. Since the disulfide bond in the SV *cyt<sub>c5</sub>* wild-type can be maintained in the oxidized state, the effects of the bond on the protein stability can be evaluated in comparison with the C59A/C62A variant in the same state. On the contrary, reduced conditions may affect *cyt c* stability through the reduced heme, as observed previously (Uchiyama et al. 2004), and also maintenance of the disulfide bond, which would give a misleading result. Therefore, the term ‘stability’ in this study simply refers the ‘stability of the oxidized protein’. The air-oxidized states of the wild-type and variant corresponded to the fully oxidized state, as confirmed by absorption spectroscopy (Fig. 4A).

Thermal denaturation curves for the SV *cyt<sub>c5</sub>* wild-type and variant were derived from

CD measurements. The data-fitted curves exhibited complete single cooperation (Fig. 6A), apparently indicating that the protein denaturation proceeded with a two-state transition. The thermal denaturation of the two proteins was reversible (> 70 %), thus providing equilibrium thermodynamic parameters (Table 1). The  $T_{m,CD}$  values were 90.3 and 67.6 °C for the wild-type and variant, respectively, indicating that the C59A/C62A variant exhibits reduced stability compared with the wild-type. The  $\Delta H_{vH}$  values (Table 1) are compared with calorimetric enthalpy changes ( $\Delta H_{cal}$ ) observed on DSC analysis below.

#### Chemical denaturation measured by CD

GdnHCl-induced denaturation curves for the SV *cytc<sub>5</sub>* wild-type and variant showed a complete two-state transition on CD analysis (Fig. 6B). The  $C_m$  value of the C59A/C62A variant (0.70 M) was smaller than that of the wild-type (1.93 M) (Table 1). The  $\Delta G_{H_2O}$  value of the wild-type was larger than that of the variant by 11.7 kJ mol<sup>-1</sup> (Table 1), indicating that the variant exhibited reduced stability during the GdnHCl denaturation similar to in the case of thermal denaturation.

#### Thermal denaturation measured by DSC

Excess molar heat capacity curves for the SV *cytc<sub>5</sub>* wild-type and C59A/C62A variant were

obtained through DSC measurements (Fig. 6C). The  $T_m$  values of the wild-type and variant were 91.1 °C and 66.9 °C, respectively (Table 1), which were close to the respective  $T_{m,CD}$  values estimated on CD analysis. Both curves well fitted the equation that represents a two-state transition for thermal denaturation (equation 1 in Appendix of ref. 28). The  $\Delta H_{cal}$  values of the SV *cyt<sub>c</sub>5* wild-type and variant at each  $T_m$ , where  $\Delta G$  equals zero, were nearly equal to the respective van't Hoff enthalpy changes ( $\Delta H_{vH}$ ) determined on CD analysis (Table 1). These results together suggest that the thermal denaturation of these proteins proceeds in a two-state manner.

From the curves of the observed excess molar heat capacity (Fig. 6B), we could obtain temperature-dependent heat capacity changes ( $\Delta C_p$ ) accompanied by the thermal denaturation. By using the  $\Delta C_p$  value at the  $T_m$  of the variant (66.9 °C),  $\Delta C_p(T_m^*)$ , other thermodynamic parameters at 66.9 °C,  $\Delta G(T_m^*)$ ,  $\Delta H(T_m^*)$ , and  $\Delta S(T_m^*)$ , could be compared for the SV *cyt<sub>c</sub>5* wild-type and variant (Table 2). Since the  $T_m$  value is defined as equivalent to the temperature at which  $\Delta G$  becomes zero, the  $\Delta G(T_m^*)$  value of the variant was zero. The wild-type  $\Delta G(T_m^*)$  value was 20.8 kJ mol<sup>-1</sup>, this being positive compared with that of the variant, indicating that the thermal stability is thermodynamically due to the disulfide bond in the SV *cyt<sub>c</sub>5* wild-type.

The  $\Delta G$  value can be dissected into enthalpy ( $\Delta H$ ) and entropy ( $\Delta S$ ) terms, as shown by

the equation,  $\Delta G = \Delta H - T\Delta S$ . The wild-type  $\Delta S(T_m^*)$  value ( $0.74 \text{ kJ mol}^{-1} \text{ K}^{-1}$ ) was only 4 % larger than that of the variant ( $0.71 \text{ kJ mol}^{-1} \text{ K}^{-1}$ ), indicating that removal of the disulfide bond has an entropic effect on protein stability in the variant (Table 2). However, the entropic disadvantage in the wild-type stability was overcome by the enthalpy term. The wild-type  $\Delta H(T_m^*)$  value ( $272 \text{ kJ mol}^{-1}$ ) more greatly contributed to the wild-type  $\Delta G(T_m^*)$  value compared with that of the variant  $\Delta H(T_m^*)$  ( $243 \text{ kJ mol}^{-1}$ ) to its  $\Delta G(T_m^*)$  value (Table 2). Comparison of these values indicates that the dominant factor stabilizing the SV *cytc<sub>5</sub>* wild-type is enthalpic. These findings are consistent with the hypothesis (Doig and Williams 1991), i.e., a disulfide bond enthalpically contributes to the protein stability.

The present results contradict the classical theory that a disulfide bond stabilizes a protein by reducing the entropy of the denatured form because the bond decreases the number of conformational states (See ref. 1 for a review). This theory is favorably applicable to a disulfide bond that closes a relatively long loop, as demonstrated previously (Pace et al. 1988; Vogl et al. 1995). SV *cytc<sub>5</sub>* has the shortest disulfide bond connection that has ever been thermodynamically characterized. Since only two amino acid residues intervene between Cys-59 and Cys-62, which form the disulfide bond in the short loop of SV *cytc<sub>5</sub>*, removal of the bond may not greatly affect the number of conformational states of the denatured form. Instead, the sulfur atoms forming the disulfide bond in the SV *cytc<sub>5</sub>* wild-type should be in

contact with the amino acid side chains near by, which enthalpically stabilize the native protein by keeping it folded tightly.

#### Structural aspects of the enthalpic contributions of the disulfide bond to SV *cyt<sub>c5</sub>* stability

From the three-dimensional structure of highly homologous ScyA, we can deduce the structural origin of the SV *cyt<sub>c5</sub>* stability caused by the disulfide bond. The aromatic ring centroid of Tyr-67 in the ScyA structure is within approximately 5 Å from the sulfur atom of Cys-62 that forms the disulfide bond with Cys-59 (Fig. 2A). Tyr-67 is also conserved in the SV *cyt<sub>c5</sub>* sequence (Fig. 1), and thus the sulfur-aromatic interaction (Reid et al. 1985) between Cys-62 and Cys-67 is one of the possible enthalpic factors stabilizing the wild-type protein. A different sulfur-aromatic interaction is also found between Cys-69 of the conserved disulfide bond and Tyr-18 in the AV *cyt<sub>c5</sub>* structure (Fig. 2B). Although Tyr-18 is not conserved at the corresponding positions of ScyA and SV *cyt<sub>c5</sub>*, and *vice versa* Tyr-67 is not in AV *cyt<sub>c5</sub>*, sulfur-aromatic interactions seem to commonly contribute to the protein stability of the class IE cyts *c*.

The ScyA structure further shows that the sulfur atoms forming the disulfide bond make contacts with the side chains of Ile-6 and Asp-65. In the SV *cyt<sub>c5</sub>* sequence, the corresponding residue to Ile-6 is Val-6 and Asp-65 is conserved (Fig. 1). These SV *cyt<sub>c5</sub>* residues are

presumably in contact with the sulfur atoms of Cys-59 and Cys-62. Therefore, the C59A/C62A mutations in SV cyt<sub>c5</sub> should cause disappearance of the van der Waals contact between the sulfur atoms and these residues, and the variant enthalpically destabilizes the native conformation. The presence of the unoccupied space with the Ala residues in the C59A/C62A variant may make the native state more accessible to the solvent. This may lead to a smaller increase in the surface area exposed upon denaturation of the variant, which correlates with the decrease in the  $\Delta C_p(T_m^*)$  value of the variant compared with that of the wild-type (Table 2). An enthalpic effect has also been shown for the human lysozyme, in which wild-type Cys-77 and Cys-95 forming a disulfide bond are substituted with Ala (Kuroki et al. 1992; Kidera et al. 1994). But, in the case of lysozyme, the  $\Delta C_p$  values did not differ between the wild-type and variant (Kuroki et al. 1992), indicating that the removal of this disulfide bond affects both the native and denatured states.

#### Effects of the disulfide bond on redox function

To examine the effects of the C59A/C62A mutations on the redox function of SV cyt<sub>c5</sub>, electrochemical experiments were carried out with CV at 25 °C. The redox potential value of the recombinant SV cyt<sub>c5</sub> wild-type was  $+309 \pm 5$  mV, which was close to the published values for authentic SV cyt<sub>c5</sub> and AV cyt<sub>c5</sub>, +301 mV (Yamada et al. 2000) and +312 mV (Carter et al.



1985), respectively. The value for the SV *cyt<sub>c5</sub>* C59A/C62A variant was  $+303 \pm 5$  mV, this being essentially the same as that of the wild-type. On the basis of consideration that a relatively high redox potential can be attributed to the hydrophobicity around the heme (Moore and Pettigrew 1990), the two SV *cyt<sub>c5</sub>* proteins, i.e., with and without the disulfide bond, may have similar heme environments. This structural consideration is supported by the present results of spectral analyses of the SV *cyt<sub>c5</sub>* wild-type and variant, in that they have the same spectral features that reflect the heme environment at the same temperature as that for the present CV measurements (Figs. 4 and 5).

Similar to the roles of the disulfide bond in the protein stability and redox function of SV *cyt<sub>c5</sub>*, the disulfide bond in *A. thaliana* *cyt c<sub>6A</sub>* contributes to the stability (Chida et al. 2006), but has no significant effect on the redox function (Wastl et al. 2004). In the *cyt c<sub>6A</sub>* structure, five amino acid residues intervene between the two Cys residues forming the disulfide bond in the 12-residue loop, instead of the two residues in the four-residue loop of SV *cyt<sub>c5</sub>*, but both loops are similarly located on the C-terminal side of the heme axial ligand of the Met residue on the polypeptide chain.

These two examples of SV *cyt<sub>c5</sub>* and *A. thaliana* *cyt c<sub>6A</sub>* are in contrast with the observations for some photosynthetic bacterial *cyts c<sub>1</sub>*, in which the disulfide bond greatly affects the redox function (Osyczka et al. 2001; Elberry et al. 2006). In these *cyts c<sub>1</sub>*, more

than 20 amino acid residues intervene between the two Cys residues forming the disulfide bond, which links one loop to another on the N-terminal side of the axial Met residue on the polypeptide chain (Berry et al. 2004; Esser et al. 2006). It will be of interest to determine whether the disulfide bond stabilizes these cyts  $c_1$ . The results should be compared with those for SV  $cytc_5$  in order to correlate thermodynamic properties with the redox function by means of the interaction involving the disulfide bond and its specific site within the  $cyt\ c$  molecule.

#### Conclusion and perspective

The short connecting disulfide bond in the loop on the C-terminal side of the axial Met residue of SV  $cytc_5$  plays a stability rather than redox role. Previously, we found that some mutations in PA  $c_{551}$ , although not related to the disulfide bond, caused changes in both protein stability and redox function (Terui et al. 2003). The present study offers another chance to regulate the stability and function of cyts  $c$ , it being possible to alter the stability without affecting the redox function.

Since the SV  $cytc_5$  C59A/C62A variant forms the wild-type-like structure at 25 °C (Figs. 4 and 5), or presumably even at a lower temperature, the SV  $cytc_5$  disulfide bond is not needed for maintenance of the structure at the physiological growth temperature of *S. violacea* (8 °C). As discussed previously (Betz 1993), the role of disulfide bonds is not limited to increasing

protein stability. The effects of the Cys-59–Cys-62 disulfide bond in SV cyt<sub>c5</sub> on its folding kinetics and reactivity with respiratory enzymes should be examined for a further insight into the roles of this short connecting disulfide bond. In addition, comparative analysis of other *Shewanella* cyt<sub>c</sub> (Fig. 1) in conjunction with mutagenesis studies will provide further knowledge on the relationship among structure, stability, and function of cyt<sub>c</sub>.

**Acknowledgements** This work was financially supported in part by grants from the Japanese Ministry of Education, Science and Culture (Grants-in-Aid for Scientific Research on Priority Areas) to Y. S. and Y.Y. (17350081), the Yazaki Memorial Foundation for Science and Technology, and the NOVARTIS Foundation (Japan) for the Promotion of Science to Y.Y.

## References

- Akiyama Y, Kamitani S, Kusukawa N, Ito K (1992) *In vitro* catalysis of oxidative folding of disulfide-bonded proteins by the *Escherichia coli dsbA* (*ppfA*) gene product. J Biol Chem 267:22440-22445
- Ambler RP (1991) Sequence variability in bacterial cytochromes *c*. Biochim Biophys Acta

1058:42-47

Arslan E, Schulz H, Zufferey R, Künzler P, Thöny-Meyer L (1998) Overproduction of the

*Bradyrhizobium japonicum* c-type cytochrome subunits of the *cbb*<sub>3</sub> oxidase in *Escherichia coli*. *Biochem Biophys Res Commun* 251:744-747

Bartalesi I, Bertini I, Hajieva P, Rosato A, Vasos PR (2002) Solution structure of a monoheme

ferrocyclochrome *c* from *Shewanella putrefaciens* and structural analysis of sequence-similar proteins: functional implications. *Biochemistry* 41:5112-5119

Berry EA, Huang LS, Saechao LK, Pon NP, Valkova-Valchanova M, Daldal F (2004) X-ray

structure of *Rhodobacter capsulatus* cytochrome *bc*<sub>1</sub>: comparison with its mitochondrial and chloroplast counterparts. *Photosynth Res* 81:251-275

Bertini I, Cavallaro G, Rosato A (2006) Cytochrome *c*: occurrence and functions. *Chem Rev*

106:90-115

Betz SF. (1993) Disulfide bonds and the stability of globular proteins. *Protein Sci* 2:1551-1558

Bonander N, Leckner J, Guo H, Karlsson BG, Sjölin L (2000) Crystal structure of the disulfide

bond-deficient azurin mutant C3A/C26A: how important is the S-S bond for folding and stability? *Eur J Biochem* 267:4511-4519

Bradford MM (1976) A rapid and sensitive method for the quantitation of microgram quantities

of protein utilizing the principle of protein-dye binding. *Anal Biochem* 72:248-254

- Brems DN, Cass R, Stellwagen E (1982) Conformational transitions of frog heart ferricytochrome *c*. *Biochemistry* 21:1488-1493
- Carter DC, Melis KA, O'Donnell SE, Burgess BK, Furey WR Jr, Wang BC, Stout CD (1985) Crystal structure of *Azotobacter* cytochrome *c*<sub>5</sub> at 2.5 Å resolution. *J Mol Biol* 184:279-295
- Chida H, Yokoyama T, Kawai F, Nakazawa A, Akazaki H, Takayama Y, Hirano T, Suruga K, Satoh T, Yamada S, Kawachi R, Unzai S, Nishio T, Park SY, Oku T (2006) Crystal structure of oxidized cytochrome *c*<sub>6A</sub> from *Arabidopsis thaliana*. *FEBS Lett* 580:3763-3768
- Doig AJ, Williams DH (1991) Is the hydrophobic effect stabilizing or destabilizing in proteins? The contribution of disulphide bonds to protein stability. *J Mol Biol* 217:389-398
- Elberry M, Yu L, Yu CA (2006) The disulfide bridge in the head domain of *Rhodobacter sphaeroides* cytochrome *c*<sub>1</sub> is needed to maintain its structural integrity. *Biochemistry* 45:4991-4997
- Esser L, Gong X, Yang S, Yu L, Yu CA, Xia D (2006) Surface-modulated motion switch: capture and release of iron-sulfur protein in the cytochrome *bc*<sub>1</sub> complex. *Proc Natl Acad Sci USA* 103:13045-13050
- Feige MJ, Hagn F, Esser J, Kessler H, Buchner J (2007) Influence of the internal disulfide bridge on the folding pathway of the C<sub>L</sub> antibody domain. *J Mol Biol* 365:1232-1244
- Goodhew CF, Brown KR, Pettigrew GW (1986) Haem staining in gels, a useful tool in the study

- of bacterial *c*-type cytochromes. *Biochim Biophys Acta* 852:288-294
- Goto Y, Hamaguchi K (1982) Unfolding and refolding of the reduced constant fragment of the immunoglobulin light chain. Kinetic role of the intrachain disulfide bond. *J Mol Biol* 156:911-926
- Guzzi R, Sportelli L, La Rosa C, Milardi D, Grasso D, Verbeet MP, Canters GW (1999) A spectroscopic and calorimetric investigation on the thermal stability of the Cys3Ala/Cys26Ala azurin mutant. *Biophys J* 77:1052-1063
- Hasegawa J, Shimahara H, Mizutani M, Uchiyama S, Arai H, Ishii M, Kobayashi Y, Ferguson SJ, Sambongi Y, Igarashi Y (1999) Stabilization of *Pseudomonas aeruginosa* cytochrome *c*<sub>551</sub> by systematic amino acid substitutions based on the structure of thermophilic *Hydrogenobacter thermophilus* cytochrome *c*<sub>552</sub>. *J Biol Chem* 274:37533-37537
- Kidera A, Inaka K, Matsushima M, Go N (1994) Response of dynamic structure to removal of a disulfide bond: normal mode refinement of C77A/C95A mutant of human lysozyme. *Protein Sci* 3:92-102
- Kuroki R, Inaka K, Taniyama Y, Kidokoro S, Matsushima M, Kikuchi M, Yutani K (1992) Enthalpic destabilization of a mutant human lysozyme lacking a disulfide bridge between cysteine-77 and cysteine-95. *Biochemistry* 31:8323-8328
- Marcaida MJ, Schlarb-Ridley BG, Worrall JAR, Wastl J, Evans TJ, Bendall DS, Luisi BF, Howe

- CJ (2006) Structure of cytochrome  $c_{6A}$ , a novel dithio-cytochrome of *Arabidopsis thaliana*, and its reactivity with plastocyanin: implications for function. *J Mol Biol* 360:968-977
- Moore GR, Pettigrew GW (1990) Cytochromes *c* – Evolutionary, structural and physicochemical aspects, Springer-Verlag, Berlin, Heidelberg
- Nogi Y, Kato C, Horikoshi K (1998) Taxonomic studies of deep-sea barophilic *Shewanella* strains and description of *Shewanella violacea* sp. nov. *Arch Microbiol* 170:331-338
- Oikawa K, Nakamura S, Sonoyama T, Ohshima A, Kobayashi Y, Takayama SJ, Yamamoto Y, Uchiyama S, Hasegawa J, Sambongi Y (2005) Five amino acid residues responsible for the high stability of *Hydrogenobacter thermophilus* cytochrome  $c_{552}$ : reciprocal mutation analysis. *J Biol Chem* 280:5527-5532
- Osyczka A, Dutton PL, Moser CC, Darrouzet E, Daldal F (2001) Controlling the functionality of cytochrome  $c_1$  redox potentials in the *Rhodobacter capsulatus*  $bc_1$  complex through disulfide anchoring of a loop and a beta-branched amino acid near the heme-ligating methionine. *Biochemistry* 40:14547-14556
- Pace CN, Grimsley GR, Thomson JA, Barnett BJ (1988) Conformational stability and activity of ribonuclease T1 with zero, one, and two intact disulfide bonds. *J Biol Chem* 263:11820-11825
- Pace CN (1990) Measuring and increasing protein stability. *Trends Biotechnol* 8:93-98

- Reid KSC, Lindley PF, Thornton JM (1985) Sulfur-aromatic interactions in proteins. FEBS Lett 190:209-213
- Sambongi Y, Stoll R, Ferguson SJ (1996) Alteration of haem-attachment and signal-cleavage sites for *Paracoccus denitrificans* cytochrome *c*<sub>550</sub> probes pathway of *c*-type cytochrome biogenesis in *Escherichia coli*. Mol Microbiol 19:1193-1204
- Sambongi Y, Uchiyama S, Kobayashi Y, Igarashi Y, Hasegawa J (2002) Cytochrome *c* from a thermophilic bacterium has provided insights into the mechanisms of protein maturation, folding, and stability. Eur J Biochem 269:3355–3361
- Swift TJ (1973) Principles and applications, In: La Mar GN, Horrocks W, DeW Jr, Holm RH (eds) NMR of paramagnetic molecules. Academic Press, New York, pp 53-83
- Terui N, Tachiiri N, Matsuo H, Hasegawa J, Uchiyama S, Kobayashi Y, Igarashi Y, Sambongi Y, Yamamoto Y (2003) Relationship between redox function and protein stability of cytochromes *c*. J Am Chem Soc 125:13650-13651
- Uchiyama S, Hasegawa J, Tanimoto Y, Moriguchi H, Mizutani M, Igarashi Y, Sambongi Y, Kobayashi Y (2002) Thermodynamic characterization of variants of mesophilic cytochrome *c* and its thermophilic counterpart. Protein Eng 15:455–461
- Uchiyama S, Ohshima A, Nakamura S, Hasegawa J, Terui N, Takayama SJ, Yamamoto Y, Sambongi Y, Kobayashi Y (2004) Complete thermal-unfolding profiles of oxidized and



- reduced cytochromes *c*. J Am Chem Soc 126:14684-14685
- Vogl T, Brengelmann R, Hinz HJ, Scharf M, Lötzbeyer M, Engels JW (1995) Mechanism of protein stabilization by disulfide bridges: calorimetric unfolding studies on disulfide-deficient mutants of the  $\alpha$ -amylase inhibitor tendamistat. J Mol Biol 254:481-496
- Wastl J, Molina-Heredia FP, Hervás M, Navarro JA, De la Rosa MA, Bendall DS, Howe CJ (2004) Redox properties of *Arabidopsis* cytochrome *c*<sub>6</sub> are independent of the loop extension specific to higher plants. Biochim Biophys Acta 1657:115-120
- Williams P, Coates L, Mohammed F, Gill R, Erskine P, Bourgeois D, Wood SP, Anthony C, Cooper JB (2006) The 1.6 Å X-ray structure of the unusual *c*-type cytochrome, cytochrome *c*<sub>L</sub>, from the methylophilic bacterium *Methylobacterium extorquens*. J Mol Biol 357:151-162
- Yamada M, Nakasone K, Tamegai H, Kato C, Usami R, Horikoshi K (2000) Pressure regulation of soluble cytochromes *c* in a deep-sea piezophilic bacterium, *Shewanella violacea*. J Bacteriol 182:2945-2952
- Zhang Y, Arai H, Sambongi Y, Igarashi Y, Kodama T (1998) Heterologous expression of *Hydrogenobacter thermophilus* cytochrome *c*-552 in the periplasm of *Pseudomonas aeruginosa*. J Ferment Bioeng 85:346-349

## Legends to Figures

**Fig. 1** Sequence comparison of *Shewanella* cytochromes *c*. Identical amino acid residues among the seven *Shewanella* cyts *c* are highlighted in grey boxes. The amino acid numbers of the seven cyts *c* are shown above the sequence of *S. violacea* DSS12 (SV cytc<sub>5</sub>). The sequence of *A. vinelandii* AvOP cyt *c*<sub>5</sub> (AV cytc<sub>5</sub>) is also shown at the bottom with the amino acid numbers below the sequence. The heme binding Cys-X-X-Cys-His sequence is shown by a horizontal bar and the conserved Cys residues forming the disulfide bond are indicated by asterisks.

**Fig. 2** Structure comparison. **a** structure of ScyA (PDB: 1KX2) of *S. oneidensis*, which was named *S. putrefaciens* in the original paper (Bartalesi et al. 2002). **b** structure of *A. vinelandii* cyt *c*<sub>5</sub> (AV cytc<sub>5</sub>, PDB: 1CC5). The main chain conformations of polypeptides are shown by grey ribbons and sulfur atoms forming the disulfide bond by black balls. The side chains of relevant Tyr residues and heme are also shown as a stick model.

**Fig 3.** Protein mobility in the SDS gel. The purified SV cytc<sub>5</sub> wild-type and C59A/C62A variant (1 µg per each lane) were treated without (–) or with (+) the reductant DTT before loading onto the SDS gels (14 % polyacrylamide). The gel was stained with Coomassie

Brilliant Blue. Molecular weight markers are also indicated.

**Fig. 4** Absorption and CD spectra. In all panels, lines represent data for the SV *cyt<sub>c5</sub>* wild-type (black line) and C59/C62A variant (grey line). **a** absorption spectra (400 – 600 nm) of air-oxidized forms (20  $\mu$ M) of the recombinant SV *cyt<sub>c5</sub>* wild-type and C59A/C62A variant. Expanded spectra (600 – 750 nm) are presented in the inset. **b** absorption spectra (400 – 600 nm) of the dithionite-reduced forms (20  $\mu$ M). **c** CD spectra (190 – 250 nm) of the air-oxidized forms (20  $\mu$ M). **d** CD spectra (250 – 400 nm) of the air-oxidized forms (100  $\mu$ M).

**Fig. 5** Paramagnetic <sup>1</sup>H NMR spectra. Spectra for the recombinant SV *cyt<sub>c5</sub>* wild-type expressed in *E. coli* (upper) and its C59A/C62A variant (lower) are shown. The corresponding relevant signals in the two spectra are connected by lines.

**Fig. 6** Thermal and GdnHCl-induced denaturation. In all panels, lines represent data for the SV *cyt<sub>c5</sub>* wild-type (black line) and C59/C62A variant (grey line). **a** thermal denaturation of SV *cyt<sub>c5</sub>* wild-type and variant was monitored by CD at 222 nm. The fraction of denaturation is shown as a function of temperature. **b** GdnHCl-induced denaturation was monitored by CD at 222 nm. The fraction of denaturation is shown as a function of the GdnHCl concentration.

Experimental data points for the SV *cyt<sub>c</sub>* wild-type (filled squares) and C59/C62A variant (open squares) are also plotted. **c** thermal denaturation was monitored by DSC. Heat capacity ( $C_p$ ) is shown as a function of temperature.

FIGURE 1. Ogawa et al.

|                                       |   |       |    |
|---------------------------------------|---|-------|----|
|                                       | 1   | 10    | 20 |
| (1) <i>S. violacea</i> DSS12          | QEGKAVYDKACHICHSMGVAGAPKAHDA                          |       |    |
| (2) <i>S. frigidimarina</i> NCIMB 400 | QEGEAIYNKACQVCHSMGVAGAPKVHDT                          |       |    |
| (3) <i>S. oneidensis</i> MR-1         | QDAEAIYNKACTVCHSMGVAGAPKSHNT                          |       |    |
| (4) <i>S. amazonensis</i> SB2B        | QEGEAVYNKACQVCHSMGVAGAPKAHDA                          |       |    |
| (5) <i>S. putrefaciens</i> CN-32      | QEAEAIYNKACTVCHSMGVAGAPKTHNT                          |       |    |
| (6) <i>S. baltica</i> OS155           | QEAEAIFNKACTVCHSMGVAGAPKVHNA                          |       |    |
| (7) <i>S. denitrificans</i> OS217     | QDGETVYNKACQVCHSMGVAGAPKVHDA                          |       |    |
| (8) <i>A. vinelandii</i> AvOP         | GGGARSGDDVVAKYCNACHGTGLLNAPKVGDS                      |       |    |
|                                       | 10  | 20    | 30 |
|                                       | 30  | 40    | 50 |
| (1)                                   | AAWEPRIAQ--GLDTLVSTVKTGKGAMPPGGMCTDCTDEDYKSAIEYMSK    | *60 * | 70 |
| (2)                                   | AAWEPRLAK--GLDALVGSVKSGLNAMPPGGMCTDCTDEDYKNAIQFMSK    |       |    |
| (3)                                   | ADWEPRLAK--GVDNLVKS VKTGLNAMPPGGMCTDCTDEDYKAAIEFMSKAK |       |    |
| (4)                                   | AQWEPRLAK--GIDALLTSVKGGLNAMPPGGMCTDCTDEDYKNAIEFMSK    |       |    |
| (5)                                   | AWEPRLAK--GIDTLLHSVKTGLNAMPPGGMCTDCTDDDYKAAIQFMSTAK   |       |    |
| (6)                                   | AWEPRLAK--GIDALLHSVKTGLNAMPPGGMCTDCTDEDYKAAIEFMSKAQ   |       |    |
| (7)                                   | AAWEPRLAK--GMDTLVASIKTGMSAMPPGGMCTDCSDEDYKNAIEFMAK    |       |    |
| (8)                                   | AAWKTRADAKGGLDGLLAQSLSGLNAMPPKGT CADCSDELKAAIGKMSGL   |       |    |
|                                       | 40  | 50    | 60 |
|                                       | 70  | 80    |    |

FIGURE 2. Ogawa et al.

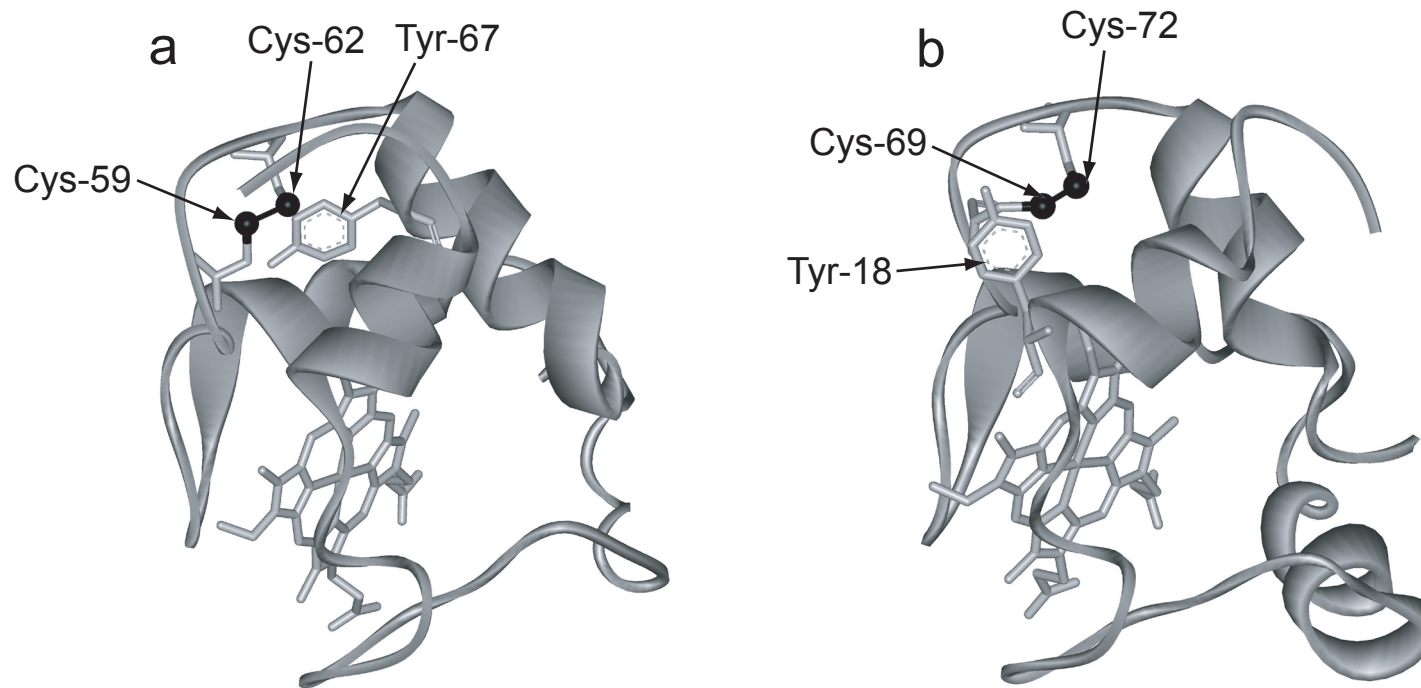


FIGURE 3. Ogawa et al.

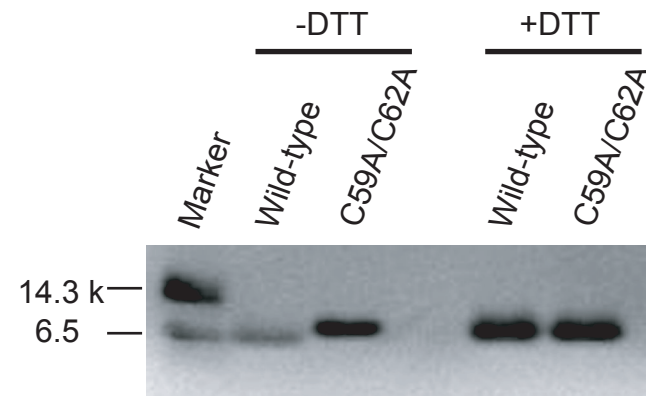


FIGURE 4. Ogawa et al.

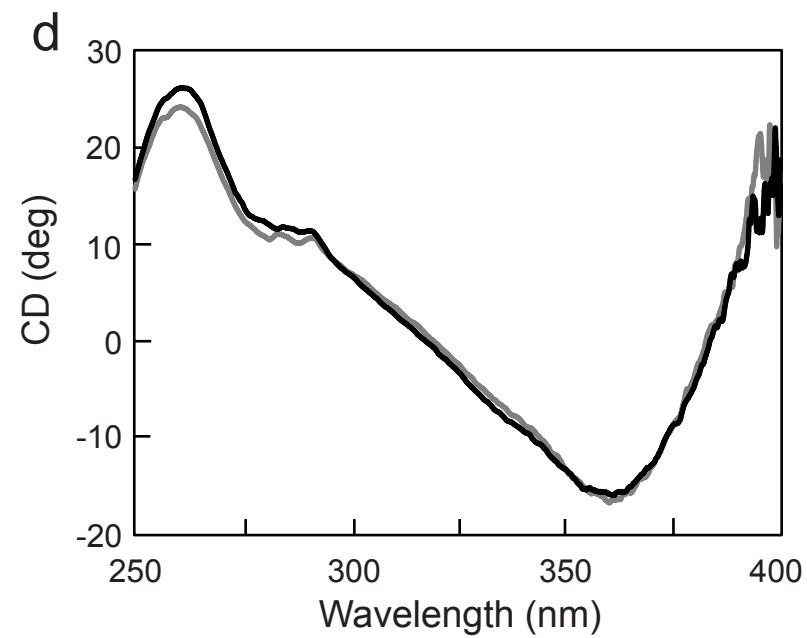
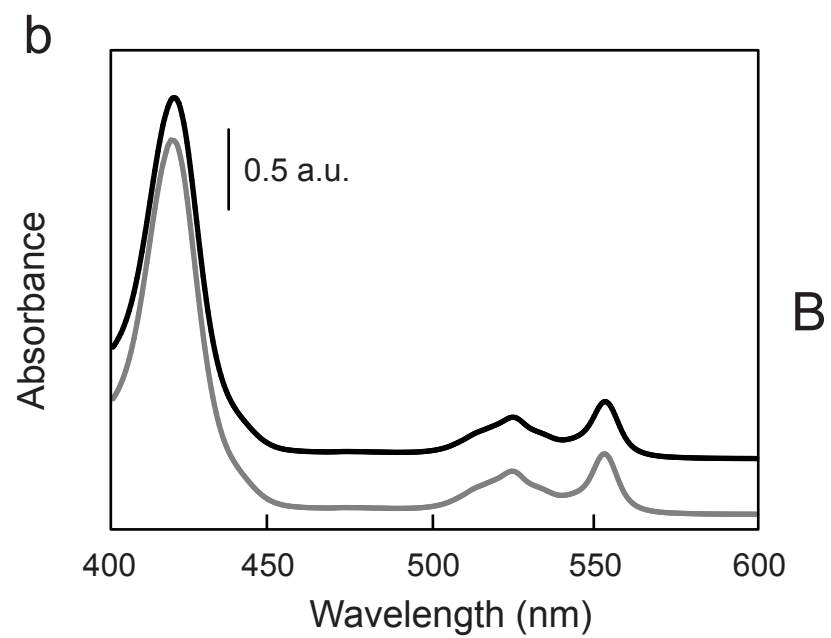
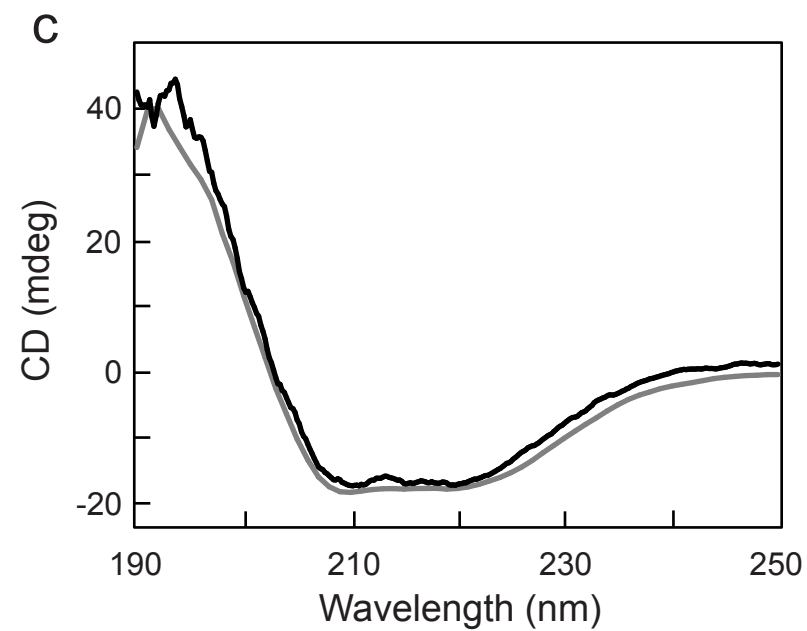
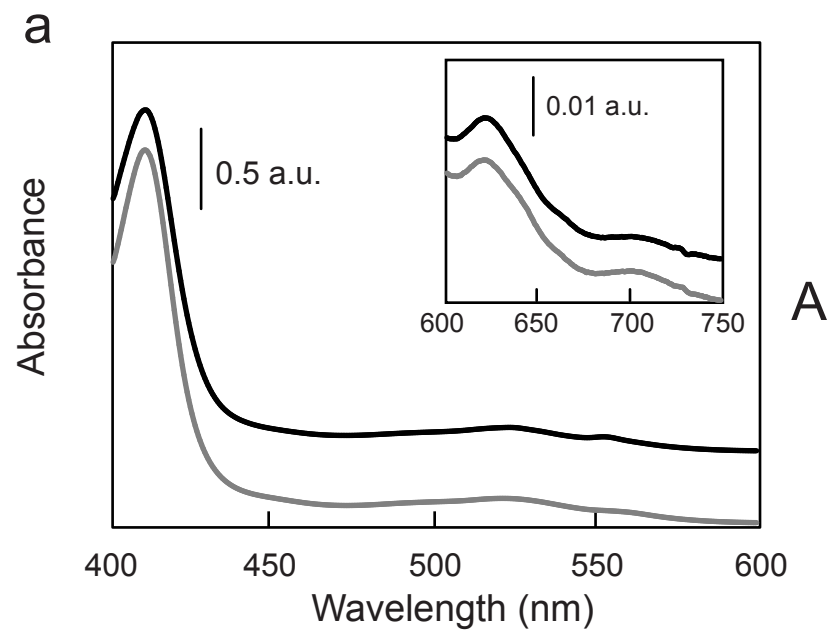




FIGURE 5. Ogawa et al.

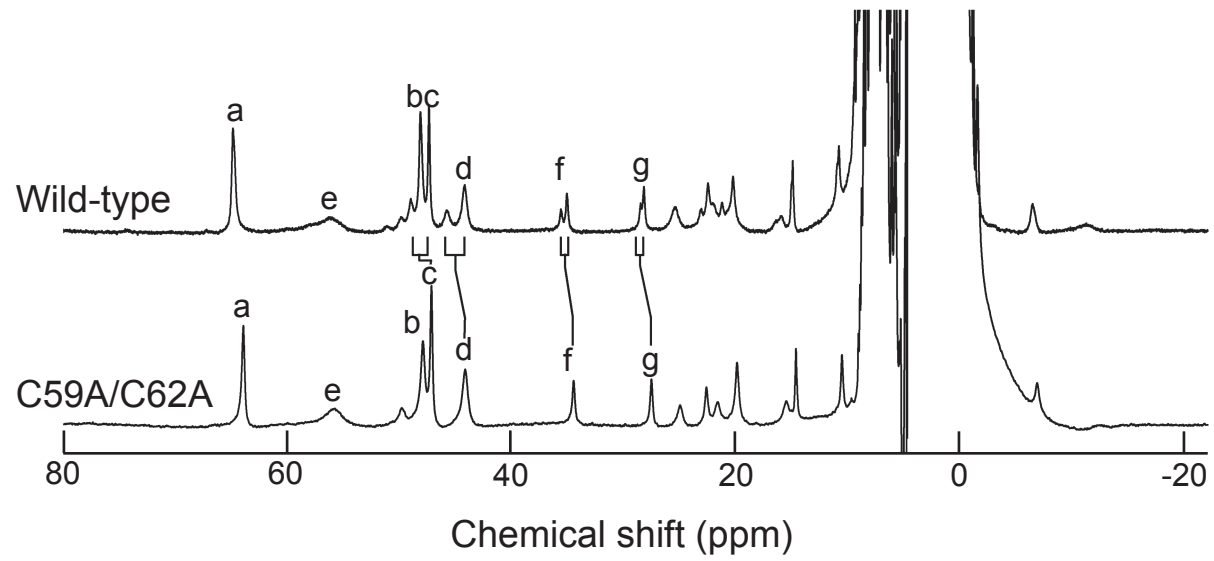


FIGURE 6. Ogawa et al.

